
Low Energy Consumption Cell Designs Involving Copper Inserts and an Innovative Busbar Network Layout

Marc Dupuis

Abstract

Two innovations presented by the authors recently at ICSOBA conferences allow to very significantly reducing both the cathode and the busbar voltage drop (Dupuis in A new aluminium electrolysis cell busbar network concept, 2015; Dupuis in New busbar network concepts taking advantage of copper collector bars to reduce Busbar weight and increase cell power efficiency, 2016). This paper combines the usage of those two innovations with the usage of the new anode stub hole design presented at the Aluminium of Siberia conference (Dupuis in Presentation of a new anode stub hole design reducing the voltage drop of the connection by 50 mV, 2016) to come up with a very low energy consumption cell design.

Keywords

MHD cell stability • Busbar design • Mathematical modeling • Power efficiency • Copper collector bars

Introduction

The author has been involved in the modeling of aluminium reduction cells for the last 30 years. In 1988, he designed the cathode of the Alcan A310 prototype cell, the first cell to operate above 300 kA in 1989. The thermo-electric cathode slice model he developed was presented at the 1991 ANSYS conference [4]. Figure 6 of that paper, reproduced in Fig. 1 shows the model mesh highlighting the cell lining and pot-shell design.

A few years later as an independent consultant, the author developed a similar demonstration model strongly inspired by the VAW CA300 cell design presented in JOM in 1994 [5]. The resulting thermo-electric cathode slice model that was first presented in Fig. 12 of the 1997 CQRDA aluminium electrolysis course [6], is reproduced in Fig. 2.

The A310 and the CA300 cells were designed at about the same time and operated at about the same amperage.

Both designers clearly respected similar design guidelines for the choice of the type of cathode blocks and side blocks, the thickness of that side block, the size of the anode to side wall distance (ASD), the location of the anode shadow, etc.

That 300 kA demonstration model typical of the early 1990s state of the art in cell design became the starting point or base case for two styles of retrofit studies, the first one aiming at minimizing the cell energy consumption presented in Dupuis [6] and the second one aiming at maximizing the cell productivity presented at the TMS 2000 conference [7]. Part of the Table 2 for a subsequent article presented in the magazine ALUMINIUM in 2005 [8] presenting the key design parameters and predicted operational results of those two cell retrofits is reproduced in Table 1.

The key design changes that are allowing either the reduction of the cell energy consumption to 12 kWh/kg or the increase of the cell productivity by 17% are the change of the type of cathode material from 30 to 100% graphitic carbon block, the reduction of the anode to cathode distance (ACD) from 5 to 4 cm and a change of the bath chemistry (and alumina feed control logic) increasing the current efficiency. Other changes are required to obtain an appropriate

M. Dupuis (✉)
GéniSim Inc., 3111 Alger St., Jonquière, QC G7S 2M9, Canada
e-mail: marc.dupuis@genisim.com

Fig. 1 Alcan A310 cathode side slice model mesh

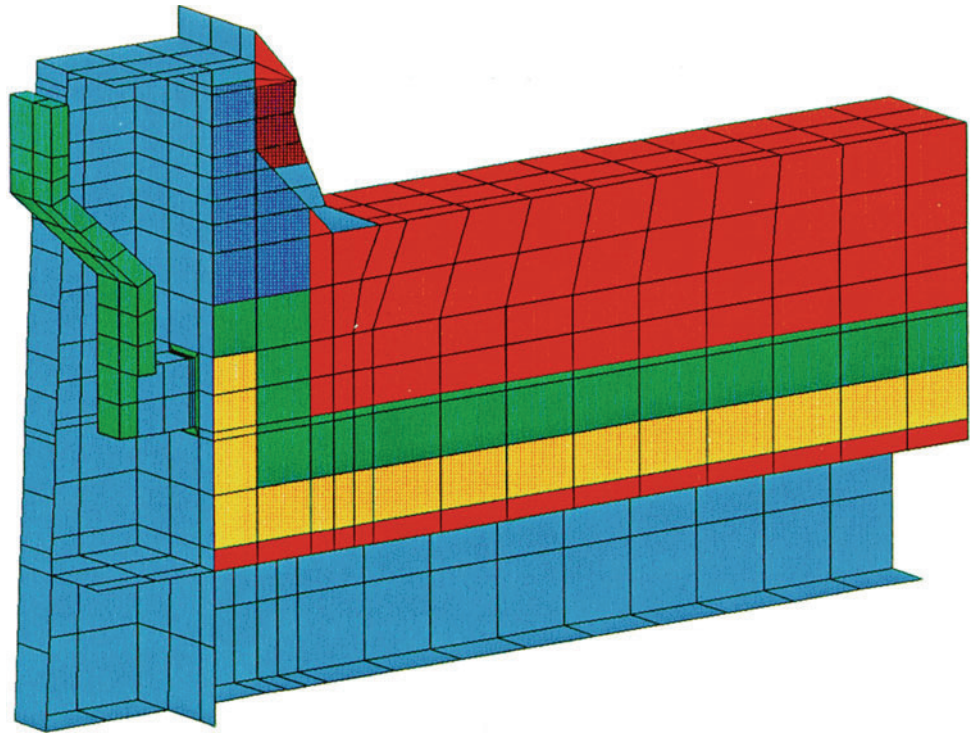


Fig. 2 VAW CA300 inspired cathode side slice model mesh

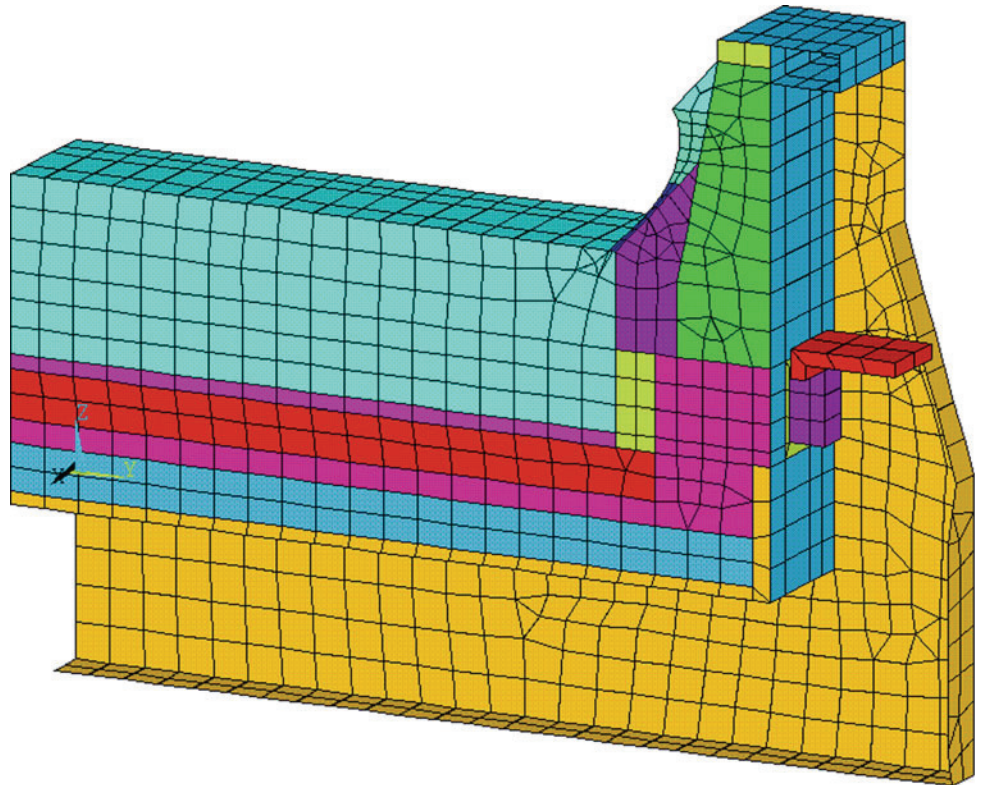


Table 1 Design and predicted operational data, part of Table 2 in Dupuis [8]

	Base case		
Amperage (kA)	300	265	350
Nb. of anodes	32	32	32
Anode size	1.6 m × 0.8 m	1.6 m × 0.8 m	1.7 m × 0.8 m
Nb. of anode studs	3 per anode	3 per anode	3 per anode
Anode stud diameter (cm)	18	16	19
Anode cover thickness (cm)	16	17.5	10
Nb. of cathode blocks	18	18	18
Cathode block length (m)	3.47	3.43	3.67
Type of cathode block	HC3	HC10	HC10
Collector bar size	20 cm × 10 cm	18 cm × 10 cm	20 cm × 10 cm
Type of side block	HC3	Anthracite	SiC
Side block thickness (cm+)	15	15	10
ASD (cm)	35	35	30
Calcium silicate thickness (cm)	3.5	6.0	3.5
Inside potshell size	14.4 × 4.35 m	14.4 × 4.35 m	14.4 × 4.35 m
ACD (cm)	5	4.15	4
Excess AlF ₃ (%)	10.90	13.50	13.50
Anode drop (mV)	303	273	323
Cathode drop (mV)	285	213	292
Anode panel heat loss (kW)	240	183	284
Cathode bottom heat loss (kW)	176	132	202
Operating temperature (°C)	973.2	956.1	960.4
Liquidus superheat (°C)	6.7	2.4	6.7
Bath ledge thickness (cm)	8.66	23.5	9.09
Metal ledge thickness (cm)	4.12	9.01	4.42
Current efficiency (%)	94.00	95.70	96.10
Internal heat(kW)	628	422	713
Energy consumption (kWh/kg)	13.72	11.93	13.43

ledge thickness at a very different level of heat dissipation. Per example, the known strategy to increase the cell productivity is to increase the anode length, decrease the ASD and use thin silicon carbide side walls. In addition, anode stud diameter and collector bar size can be increased while the anode cover thickness can be decreased.

The design strategy to decrease the cell energy consumption to 12 kWh/kg is the opposite, anode stud diameter and collector bar size can be decreased while the anode cover thickness can be increased. What is a lot more significant is that the cell productivity must be decreased by 12%, which explains why so far the industry have not move in that direction despite the fact that operation at that level of power efficiency have been reported as soon as the early 80s [9, 10].

Clearly, a cell designer cannot at the same time aim at maximizing the cell productivity and minimizing the cell energy consumption. This is why Rio Tinto per example has

developed and is offering both the AP60 and the APXe cells based on the same basic platform [11].

Yet, new choice of materials and new and innovative design ideas can always be put to contribution in order to further increase the cell productivity or decrease the cell energy consumption. Another tendency is to continue to increase the cell size in order to keep reducing both the cell OPEX and CAPEX. It is in that context that the AP60 platform replaced the AP30 platform that itself replaced the AP18 platform [12] per example.

For one, the author have been advocating that, despite the difficulties that have always been limiting the rate of increase of the cells size since the beginning of the industry, he could foresee no technical limitation that could limit further increase of cell size in the future. It is in that context that the author presented a 500 kA cell design in 2003 in Dupuis [13] and a 740 kA cell design in 2005 in Dupuis [8].

In yet another cell retrofit demonstration study paper in 2011 [14] the author took advantage of new design innovations like collector bar copper inserts, anode slots and a new type of anode stub hole design [3] to retrofit the 500 kA cell presented in Dupuis [13] into a more productive 600 kA cell operating at about the same power efficiency. As an intermediary step, not quite optimized in term of thermal conditions, a 500 kA cell operating at 12.1 kWh/kg was also developed. Table 2 presents detailed data of that study.

New Retrofit Study Aiming at Minimizing Cell Energy Consumption Even Further

In the past 30 years, the market conditions of high metal value and the existence of regions of the world offering inexpensive electrical power were favorable for new cell

designs maximizing cell productivity while maintaining power efficiency in the 13–13.5 kWh/kg range.

The market conditions have evolved recently to a much lower metal value and far less availability of inexpensive electrical power. In that context, the metal production cost is getting quite close to the metal market value and a reduction of the energy consumption can make the difference between operating at profit or at loss.

Technically, 12–12.5 kWh/kg have been achieved multiple times and as for operation at 13–13.5 kWh/kg range, under the current market conditions it might well become the preferable operational range. The next question is technically, regardless of market conditions, how much lower can we manage to go?

Reducing the cell energy consumption means reducing the cell voltage drop which in turn means reducing the cell ohmic resistance. This statement assumed that at 95–96% current efficiency, we cannot expect significant gain to come

Table 2 Design and predicted operational data, original work presented in Dupuis and Bojarevics [14]

	Base case		
Amperage (kA)	500	500	600
Nb. of anodes	40	48	48
Anode size	1.95 m × 0.8 m	1.95 m × 0.665 m	2.0 m × 0.665 m
Nb. of anode studs	3 per anode	4 per anode	4 per anode
Anode stud diameter (cm)	20.5	17.5	17.5
Anode cover thickness (cm)	10	10	10
Nb. of cathode blocks	24	24	24
Cathode block length (m)	4.17	4.17	4.17
Type of cathode block	HC10	HC10	HC10
Collector bar size	20 cm × 10 cm	20 cm × 10 cm	20 cm × 10 cm
Type of side block	SiC	SiC	SiC
Side block thickness (cm+)	10	10	7
ASD	30	30	28
Calcium silicate thickness (cm)	3.5	3.5	3.5
Inside potshell size	17.8 × 4.85 m	17.8 × 4.85 m	17.8 × 4.85 m
ACD (cm)	4	3.5	3.5
Excess AlF ₃ (%)	13.50	12.00	12.00
Anode drop (mV)	354	265	318
Cathode drop (mV)	314	87	104
Anode panel heat loss (kW)	409	420	449
Cathode bottom heat loss (kW)	273	238	240
Operating temperature (°C)	963.1	955.6	964.8
Liquidus superheat (°C)	9.4	2.6	11.8
Bath ledge thickness (cm)	6.15	29	4.76
Metal ledge thickness (cm)	2.42	26	1.07
Current efficiency (%)	95.90	96.50	96.40
Internal heat (kW)	1043	760	1140
Energy consumption (kWh/kg)	13.61	12.1	13.26

from that factor. Leaving aside the bath ohmic resistance for now, this leaves three distinct ohmic resistances to work with: the anode, cathode and busbar resistances.

Cathode Design with Copper Collector Bars

As presented in Table 2, the intermediary cell operating at 500 kA presented in Dupuis and Bojarevics [14] was operating at 87 mV at cathode drop by using the copper collector bars design presented in Fig. 3.

At the time, it was speculative that such a collector bar design could be actually build, but it is no longer the case today after Storvik AS presentation at the ISCOBA 2015 conference [15]. Furthermore, at the TMS 2016 conference KAN-NAK advocated that copper collector bars don't even need to be protected by a shell of steel [16].

As first presented in Dupuis [2], what the author did not realized in 2011 is that with the usage of copper collector bars, 100% of the cell current can be extracted on the downstream side without generating excessive horizontal current in the metal pad or producing excessive cathode voltage drop.

The results presented in Dupuis and Bojarevics [14] and in Dupuis [2] are for a 20 cm × 10 cm copper collector bar size. When the current is extracted all on the downstream side of that cell running at 500 kA, the current density in the bar doubles, and the cathode voltage drop increases from 87 to 174 mV as presented in Dupuis [2].

New results for a bigger 25 cm × 16 cm copper collector bar are presented here. As can be seen in Fig. 4, the cathode voltage drop is reduced back to 130 mV.

Figure 5 presents the horizontal currents in the metal pad. They have been reduced as compared to those presented in Fig. 2 of Dupuis [2]. Unfortunately, the center channel

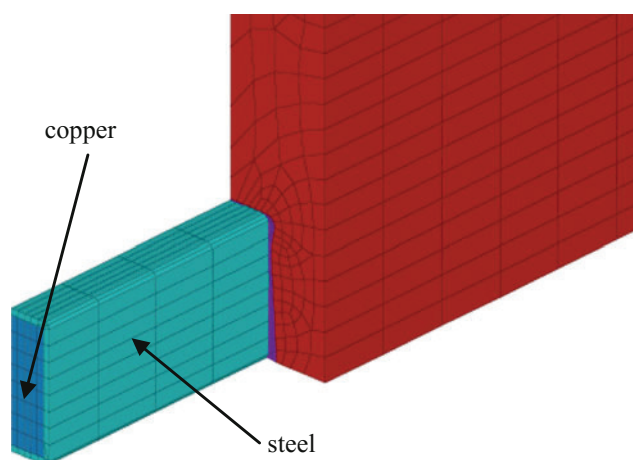


Fig. 3 Copper collector bar design originally proposed in Dupuis and Bojarevics [14]

creates a gap that prevents the total elimination of a horizontal component in the metal pad current regardless of the size of the copper collector bars used.

External Compensation Current (ECC) Busbar Network Design

As presented in Dupuis [2], the idea of taking advantage of copper collector bars to extract 100% of the cell current on its downstream side came to the author as a way to reduce of busbar weight of its own reversed compensation current (RCC) busbar configuration.

It happens that the same idea is easily applicable to existing ECC busbar configurations. In that case, the busbar network is reduced to only the anode risers so it is the preferable busbar configuration if the main goal is to minimize the busbar voltage drop in order to minimize the cell energy consumption.

Figure 6 presents the busbar network and the calculated busbar drop of 134 mV. The busbar current density is quite low but this is consistent with a business scenario where the metal cost is low and the energy cost is high. Figure 7 is presenting the vertical component of the magnetic field (B_z) obtained while using this busbar configuration (see [2] for more results).

Anode Design with Innovative Stub Hole Conception

As presented in Dupuis and Bojarevics [14] and in Table 2, when operating the cell at 500 kA using 48 anodes of 1.95 m × 0.665 m, the predicted voltage drop is 265 mV. This already very low anode drop is in great part due to the usage of an innovative stub hole conception. That innovative conception was tested in a thermo-electro-mechanical (TEM) model presented in Dupuis [17]. Figure 4 of Dupuis and Bojarevics [14] is showing the voltage drop prediction from that TEM model but not the new stub hole design investigated.

That design has been presented for the first time in Dupuis [3]. Figure 8 is presenting the original ANSYS voltage drop figure of the TEM model testing that new stub hole design concept.

As discussed in Dupuis [3], the aim of the new design is to get a good contact pressure between the stub bottom horizontal face and the anode stub hole bottom horizontal face. This is achieved by locking the stub vertical thermal expansion. As presented in Dupuis [3], there is more that one way to achieve this, the final optimized shape presented in Dupuis [3] is less costly to implement, but was developed after [14] was written.

Fig. 4 Cathode voltage drop

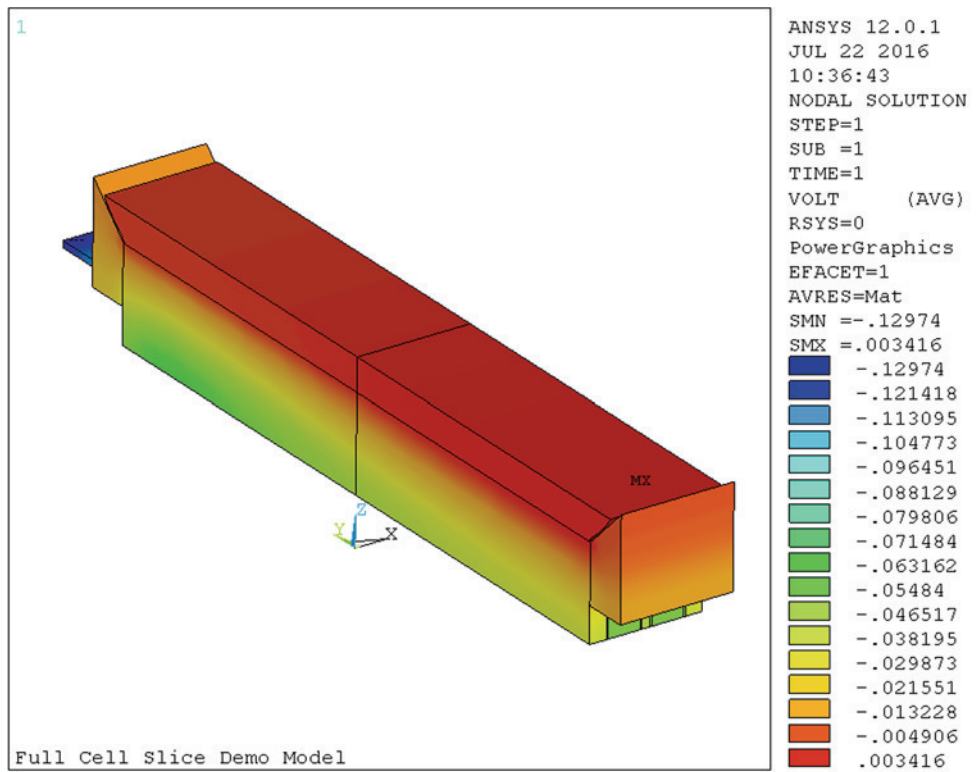


Fig. 5 Metal pad current density

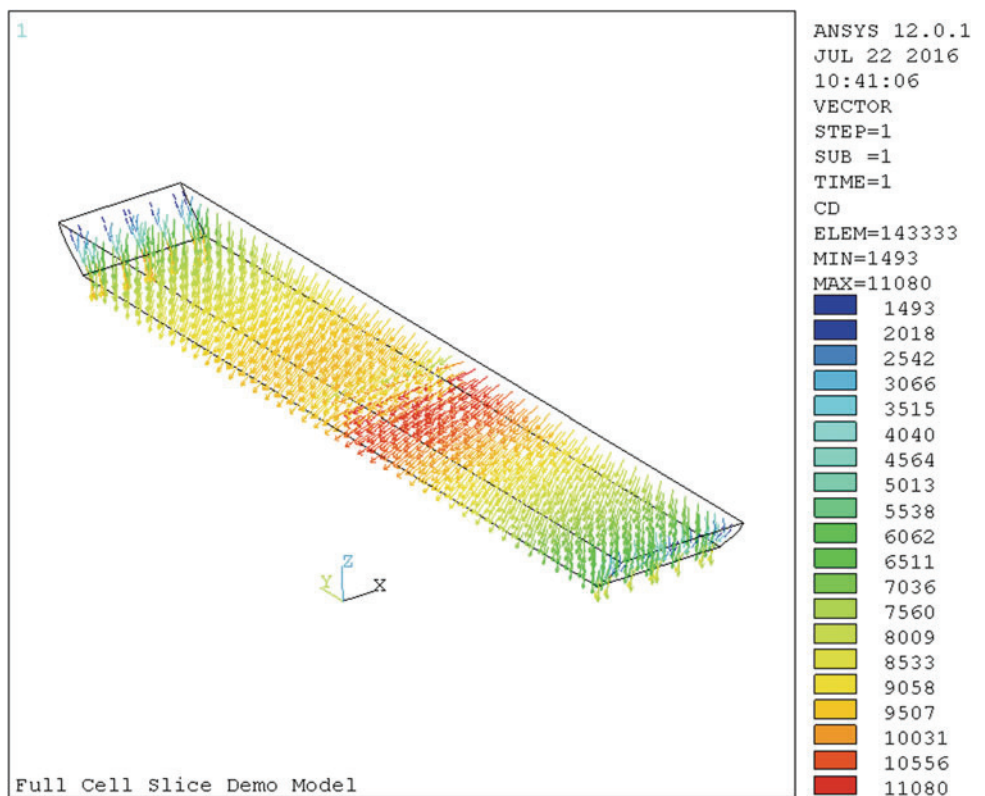


Fig. 6 Busbar drop of the ECC busbar network concept with 100% downstream side current exit

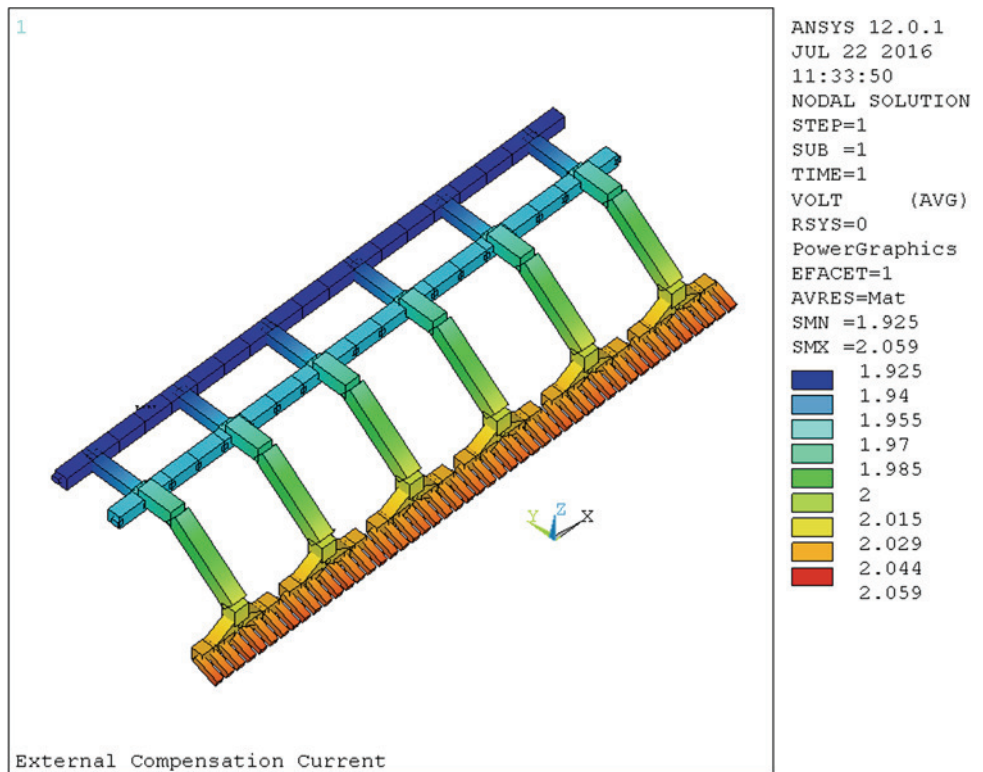
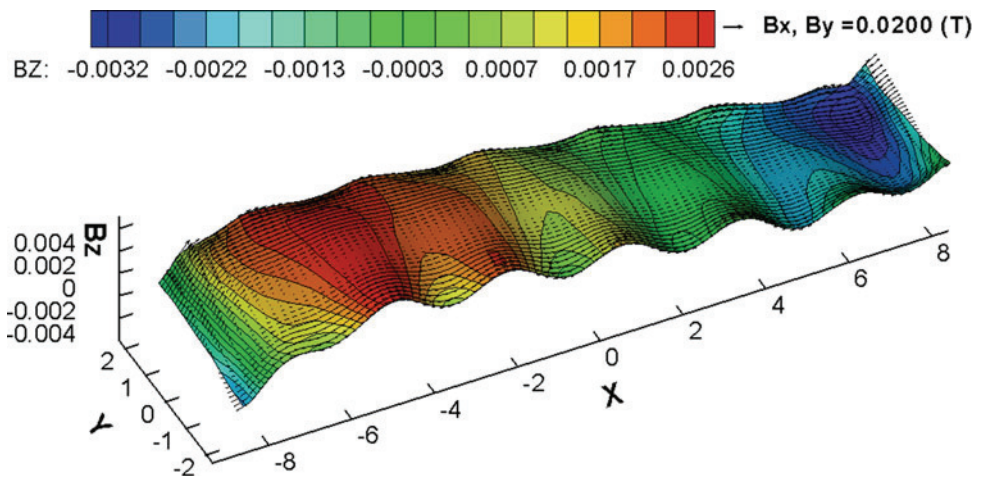


Fig. 7 Vertical component of the magnetic field (B_z), Fig. 10 in Dupuis [2]



From that starting point, the author tried to further reduce that anode voltage drop for this study. The option to add copper insert like the one presented in Sverre Sæsbøe [15] was investigated but the gains were disappointing. It turned out that the best way to achieve more mV saving was to improved the anode aspect ratio.

Figure 9 is presenting the current anode aspect ratio, each stub is feeding a rectangular carbon section of $0.4875 \text{ m} \times 0.665 \text{ m}$, and ideally, each stub should be feeding a square section of carbon. This is important since

with 4 fairly big stubs and the new stub hole design, the biggest resistance is now in the carbon section of the anode.

For that reason, the 48 $1.95 \text{ m} \times 0.665 \text{ m}$ anodes have been replaced with 64 $1.95 \text{ m} \times 0.5 \text{ m}$ anodes keeping the exact same stub diameter and stub hole design in order to avoid to go back running the TEM model. Figure 10 presents the new anode aspect ratio.

With a parametric model at your disposal, the half anode model can be modified in no time. The same is true for the full anode panel model. Figure 11 is presenting the initial

Fig. 8 Anode voltage drop from the TEM model

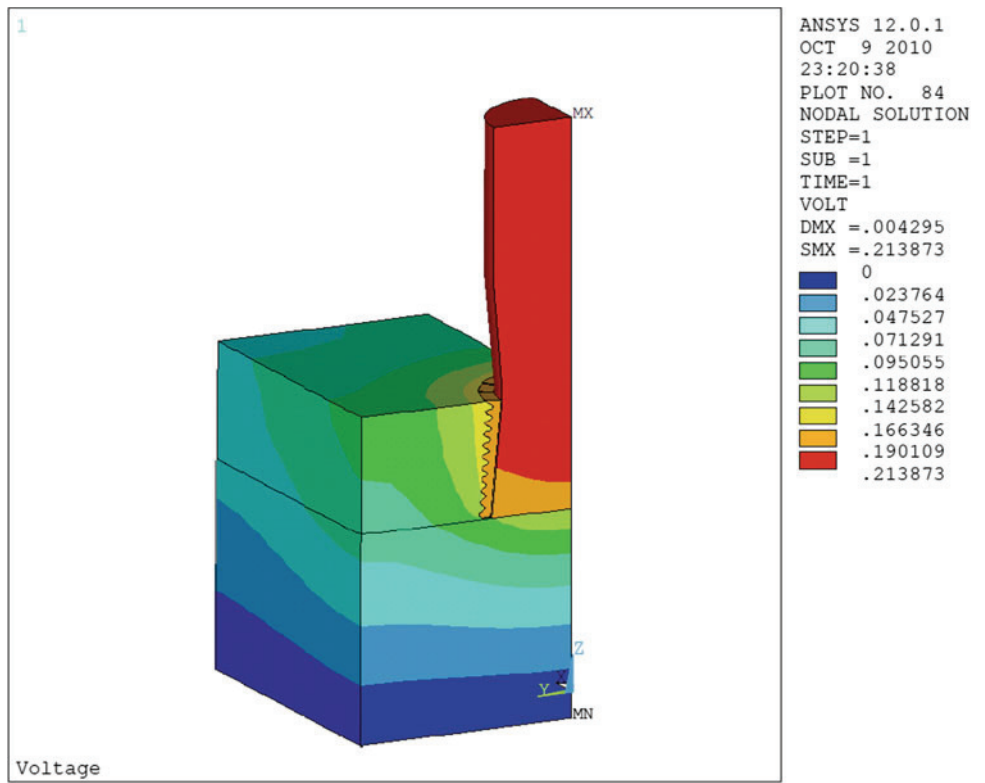


Fig. 9 One of the 48
 1.95 m × 0.665 m anode

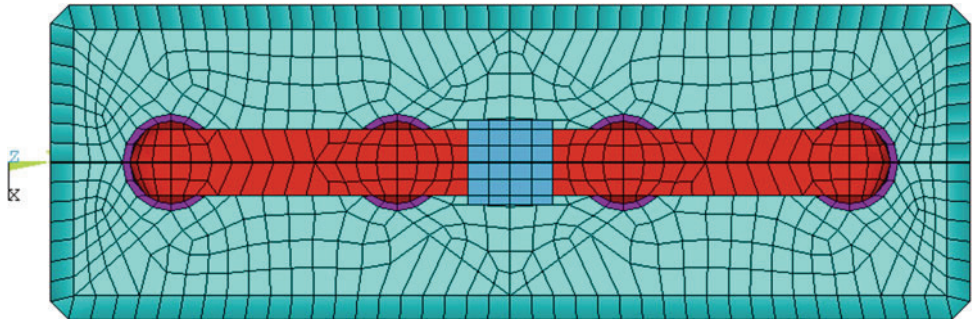
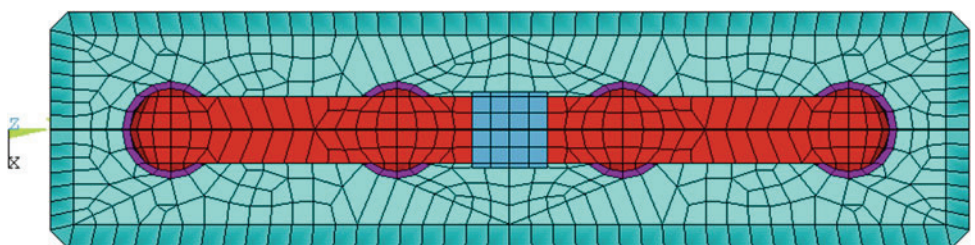


Fig. 10 One of the 64
 1.95 m × 0.5 m anode



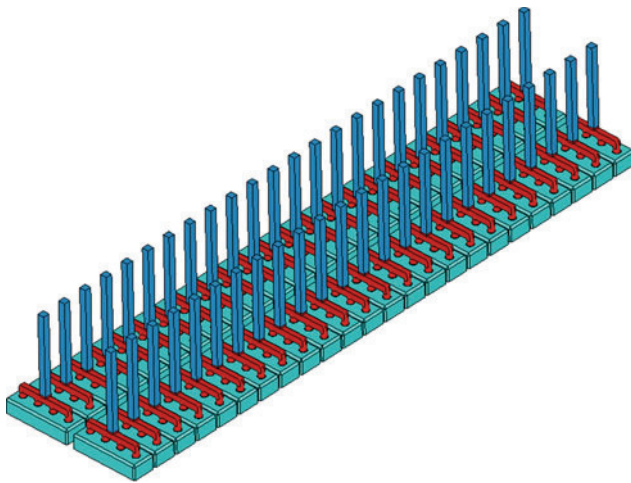


Fig. 11 48 anodes panel layout

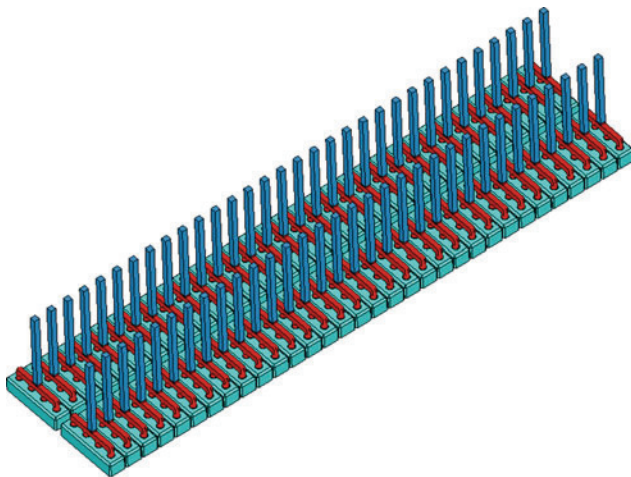


Fig. 12 64 anodes panel layout

48 anodes panel layout while Fig. 12 is presenting the new 64 anodes panel layout.

The resulting anode voltage drop is presented in Fig. 13, simply by changing the anode aspect ratio and by increasing the number of anodes from 48 to 64, the anode voltage drop has been reduced from 265 to 224 mV.

Calculation of the Resulting Cell Energy Consumption

Several modeling tools could be used to calculate the cell energy consumption from the above results. In Dupuis and Bojarevics [14] the author used Dyna/Marc [18] which also predicts the cell superheat and corresponding ledge thickness.

So far no effort has been made to adjust the cell lining design to the new cell operating conditions so a simple cell voltage break down tool like Peter Entner's CellVolt [19] was used instead. Table 3 presents the results obtained for the operation at 500 kA corresponding to running at 0.8 A/cm^2 of anode current density.

As in Dupuis [2], the calculation was done using 3.2 cm of ACD instead of 3.5 cm used in Dupuis and Bojarevics [14] as since 2011, indications are that ACD have been reduced further more in low energy consumption cell prototypes. At 3.2 cm ACD, the predicted cell energy consumption is calculated to be 11.2 kWh/kg.

More significantly, the cell internal heat is calculated to be only 699 kW while the cell lining was designed to comfortably dissipate 1140 kW with $20 \text{ cm} \times 10 \text{ cm}$ size collector bars and 192 anode stubs. Clearly a very serious cell lining redesign work needs to be performed as the next step. New insulating materials like the ceramic fire board extensively used in Zhou and Dupuis [20] will certainly need to be added to the list of lining materials.

In order to make the new cell lining design work even more challenging and the cell energy savings even more impressive, Table 3 also reports results for an operation at 400 kA corresponding to running at only 0.64 A/cm^2 of anode current density. At that current density and still at 3.2 ACD, the cell is expected to produce metal using only 9.95 kWh/kg.

The corresponding cell internal heat is calculated to be reduced to 414 kW which is only 36% of the 1140 kW dissipated by the same cell "platform" running at 600 kA and 13.26 kWh/kg.

Fig. 13 Anode voltage drop from the TE model

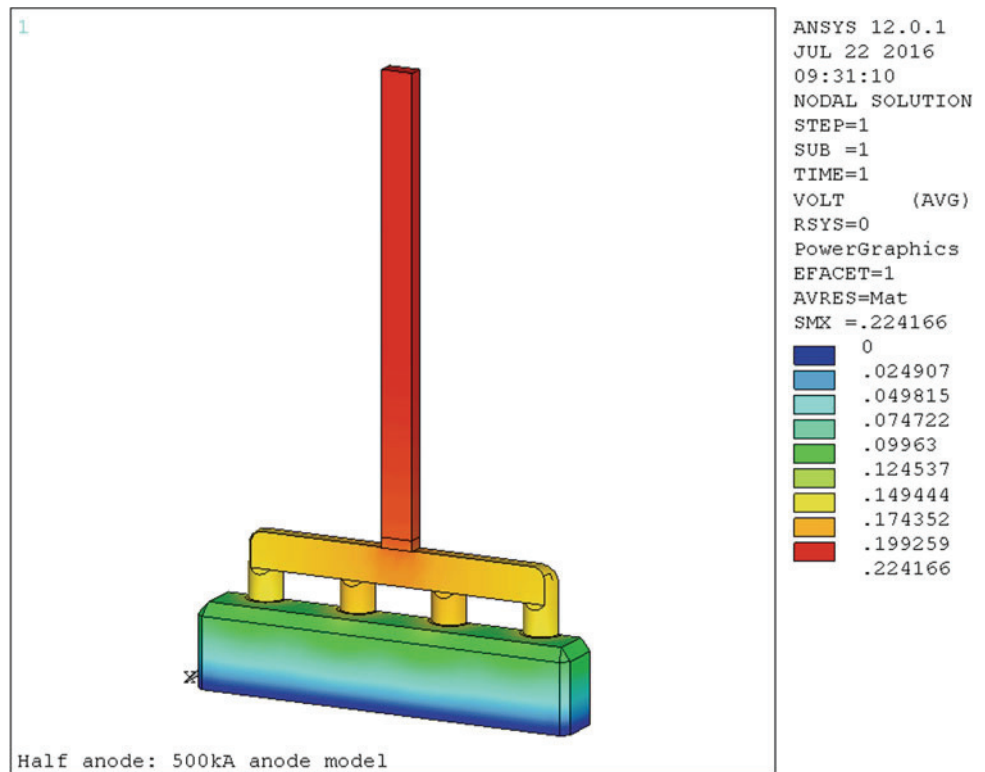


Table 3 Design and predicted cell energy consumption

	Base case		
Amperage (kA)	500	500	400
Nb. of anodes	48	64	64
Anode size	1.95 m × 0.665 m	1.95 m × 0.5 m	1.95 m × 0.5 m
Nb. of anode studs	4 per anode	4 per anode	4 per anode
Anode stud diameter (cm)	17.5	17.5	17.5
Anode cover thickness (cm)	10	10	10
Nb. of cathode blocks	24	24	24
Cathode block length (m)	4.17	4.17	4.17
Type of cathode block	HC10	HC10	HC10
Collector bar size	20 cm × 10 cm	25 cm × 16 cm	25 cm × 16 cm
Type of side block	SiC	SiC	SiC
Side block thickness (cm+)	10	10	10
ASD (cm)	30	30	30
Calcium silicate thickness (cm)	3.5	3.5	3.5
Inside potshell size	17.8 × 4.85 m	17.8 × 4.85 m	17.8 × 4.85 m
ACD (cm)	3.5	3.2	3.2
Excess AlF ₃ (%)	12.00	12.00	12.00
Anode drop (mV)	265	224	179
Cathode drop (mV)	87	130	104
Busbar drop (mV)	310	134	107
Cell voltage (V)	3.89	3.59	3.20
Current efficiency (%)	95.90	95.90	95.90
Internal heat (kW)	758	699	414
Energy consumption (kWh/kg)	12.1	11.2	9.95

Conclusions

Two innovations presented by the authors recently at ICSOBA conferences allow to very significantly reducing both the cathode and the busbar voltage drop:

- cathode design with copper collector bars extracting 100% of the cell current on its downstream side
- the usage of modified external compensation current (ECC) busbar configuration made only of anode risers;

are combined with a third innovation presented at the Aluminium of Siberia conference:

- the usage of a new anode stub hole design.

As a result, a cell operating at 500 kA, 0.8 A/cm² of anode current density and 3.2 cm ACD is predicted to have an energy consumption of about 11.2 kWh/kg.

The same cell platform operating at 400 kA, 0.64 A/cm² of anode current density and 3.2 cm ACD is predicted to have an energy consumption of about 9.95 kWh/kg.

References

1. M. Dupuis, A new aluminium electrolysis cell busbar network concept. in *Proceedings of 33rd International ICSOBA Conference, Travaux No. 44, Dubai, UAE, 29 Nov–1 Dec 2015, Paper AL21*
2. M. Dupuis, New busbar network concepts taking advantage of copper collector bars to reduce busbar weight and increase cell power efficiency. in *Proceedings of 34th International ICSOBA Conference, Travaux No. 45, Quebec, Canada, 2–5 Oct 2016 (to be published)*
3. M. Dupuis, Presentation of a new anode stub hole design reducing the voltage drop of the connection by 50 mV. in VIII International Congress and Exhibition “Non-Ferrous Metals and Minerals”, Krasnoyarsk, Russia, 13–16 Sept 2016 (to be published)
4. M. Dupuis, I. Tabsh, Thermo electric coupled field analysis of aluminum reduction cells using the ANSYS parametric design language. in *Proceeding of the ANSYS® Fifth International Conference, vol 3. (1991), pp. 17.80–17.92*
5. V.A. Kryukovski, G.A. Sirasutdinov, J. Klein, G. Peychal-Heiling, International cooperation and high-performance reduction in Siberia. *JOM* **46**(2), 23–25 (1994)
6. M. Dupuis, Les modèles thermiques. in *2e Symposium québécois sur le procédé d'électrolyse de l'aluminium, CQRDA, 1997*
7. M. Dupuis, Thermo-electric design of a 400 kA cell using mathematical models: a tutorial. *TMS Light Metals* (2000), pp. 297–302
8. M. Dupuis, Thermo-electric design of a 740 kA cell, is there a size limit. *Aluminium* **81**(4), 324–327 (2005)
9. O. Fujishima, M. Takasawa, K. Wakaizumi, Advanced energy saving in aluminum reduction cell. *AIME Light Met.* (1982), pp. 559–569
10. S. Tanji, O. Fujishima, K. Mori, Substantial energy saving in existing potlines. *AIME Light Met.* (1983), pp. 577–586
11. AP60 and APXe: a breakthrough in productivity, energy consumption and emissions. AP Technology™ Fact sheet, Mar 2015
12. F. Charmier, O. Martin, R. Gariépy, Development of the AP technology through time. *JOM* **67**(2), 336–341 (2015)
13. M. Dupuis, Thermo-electric design of a 500 kA cell. *Aluminium* **79**(7/8), 629–631 (2003)
14. M. Dupuis, V. Bojarevics, Retrofit of a 500 kA cell design into a 600 kA cell design. *Aluminium* **87**(1/2), 52–55 (2011)
15. D. Sverre Sæsbøe, Storvik high conductivity anode yoke with copper core. in *Proceedings of 33rd International ICSOBA Conference, Travaux No. 44, Dubai, UAE, 29 November–1 December 2015, Paper AL23*
16. R. von Kaenel and al., Copper bars for the Hall-Héroult process. *TMS Light Met.* 2016, 903–908
17. M. Dupuis, “Development and application of an ANSYS based thermo-electro-mechanical anode stub hole design tool”, *TMS Light Metals*, 433–438 (2010)
18. M. Dupuis, H. Côté, Dyna/Marc 14.0 user's guide. *GeniSim* (2012)
19. P. Entner, CellVolt AIWeb application: <http://peter-entner.com/ug/windows/cellvolt/toc.aspx>
20. J. Zhou, M. Dupuis, In-depth analysis of lining designs for several 420 kA electrolytic cells. *TMS Light Met.*, 685–690 (2015)